Considerations for the delivery of STING ligands in cancer immunotherapy

Petrovic, Marija; Borchard, Gerrit; Jordan, Olivier

How to cite

PETROVIC, Marija, BORCHARD, Gerrit, JORDAN, Olivier. Considerations for the delivery of STING ligands in cancer immunotherapy. In: Journal of controlled release, 2021, vol. 339, p. 235–247. doi: 10.1016/j.jconrel.2021.09.033

This publication URL: https://archive-ouverte.unige.ch/unige:157083
Publication DOI: 10.1016/j.jconrel.2021.09.033

Journal of Controlled Release 339 (2021) 235–247

Contents lists available at ScienceDirect

Journal of Controlled Release

journal homepage: www.elsevier.com/locate/jconrel

Considerations for the delivery of STING ligands in cancer immunotherapy

M. Petrovic, G. Borchard, O. Jordan *

Institute of Pharmaceutical Sciences of Western Switzerland (ISPSO), Section of Pharmaceutical Sciences, University of Geneva, Switzerland

ARTICLE INFO

Keywords:
cGAS-STING
cGAMP
STING
Immunotherapy
APC
Nanoparticles
Microparticles

ABSTRACT

Several studies have shown the importance of the cGAS-STING pathway in antigen-presenting cells for anti-cancer immunity. Cyclic GMP-AMP (cGAMP) – STING ligand is a negatively charged dinucleotide prone to degradation by hydrolases. Once administered in its soluble form, high doses are needed which in turn may cause side effects such as T cell apoptosis. Moreover, due to its negative charge, transfection of cGAMP into negatively-charged membrane cells is hampered. In order to achieve successful transfection and protection from enzymatic degradation there is a need for a suitable carrier for cGAMP. In this review, we therefore describe currently reported carriers for cGAMP, and correlate their characteristics to the effect they cause. To achieve targeted delivery to the tumor microenvironment, the route of administration and physicochemical parameters of the particles (containing a carrier and cGAMP) such as size and charge need to be determined. Therefore, the choice of the particle formulation and its impact on the preclinical outcome will be discussed.

1. Introduction

Immunotherapy is a recently developed, effective therapeutic strategy against cancer employing the activation of innate and adaptive immunity of the patient. The stimulator of interferon genes (STING) pathway, as a part of the innate immune system is a pattern recognition receptor (PRRs), more specifically cytosolic DNA sensor. Once it is activated by cytosolic dsDNA (double stranded microbial or tumor DNA), interferon type I (type I IFN) is produced within the cell, followed by release and activation of dendritic cells (DC), which in turn will activate tumor specific CD8+ T cells. As a result, activation of this pathway results in bridging and tight synergy between innate and adaptive immunity [1,2]. Due to malignant transformation, an abnormal formation of chromatin fragments is occurring, and possible leakage of DNA into the cytosol of the cancer cell or uptake by DC [3]. Besides dendritic cells, the STING pathway is conserved in many other cell types, but so far, the most relevant cells having an antitumor activity are antigen-presenting cells (APCs) such as DC and macrophages [4]. Depending on the type of the macrophages surrounding the tumor mass and the extent of immune cell infiltration, it is possible to determine the tumor microenvironment (TME) status. If the TME lacks immune cell infiltration and consists of tumor-associated macrophages (TAMs), which phenotypically resemble M2 macrophages responsible for immune-suppression, the TME is defined as "cold" or poorly immunogenic. On the contrary, "hot" TME, besides immune cell infiltration, displays classical M1 macrophages having a beneficial effect on tumor regression and an overall better prognosis [5]. It was shown that the STING pathway might be responsible for shifting the macrophage phenotype from M2 towards M1, as will be further detailed in this review [6,7]. Additionally, activation of STING pathway confirmed an increased programmed cell death 1 ligand (PD-L1) receptor expression in tumor cells [8]. Overall, the STING pathway likely represents a novel favorable target for cancer immunotherapy, promoting tumor infiltration by CD 8+ T cells, macrophages shifting from M2 to M1 phenotype

Abbreviations: IFN type I, interferon type I IFN type I; PRRs, pattern recognition receptors; DC, dendritic cells; APC, antigen-presenting cells; TME, tumor microenvironment; TAAs, tumor-associated antigens; TAMs, tumor-associated macrophages; PD – L1, programmed cell death 1 ligand; CDN, Cyclic dinucleotide; cGAMP, cyclic GMP-AMP; cGAS, Cyclic GMP–AMP synthase; dsDNA, double stranded; ER, endoplasmic reticulum; TBK1, TANK-binding kinase 1; IRF 3, interferon regulatory transcription factor 3; NF-κB, nuclear factor kappa-light-chain-enhancer of activated B cells; NK, natural killer cell; TDLN, tumor-draining lymph nodes; MEFs, mouse embryonic fibroblasts; CTL, cytotoxic lymphocyte; TLS, tertiary lymphoid structures; ICB, Immune checkpoint blockade; CTLA-4, cytotoxic T-lymphocyte-associated Protein **4**; ENPP1, hydrolase ectonucleotide pyrophosphatase; RC, receptor; FcRs, Fc receptors; RES, reticuloendothelial system; PAMPs, Pathogen-associated molecular patterns; FDA, Food and Drug Administration; MPs, micro particles; TNBC, Triple-negative breast cancer; PLGA, polylactic-co-glycolic acid; UPS, ultra-pH sensitive; ROS, reactive oxygen species; CSiNPs, cationic silica nanoparticles; HNSCC, head and neck squamous cell carcinoma.

* Corresponding author.
E-mail address: Olivier.jordan@unige.ch (O. Jordan).

https://doi.org/10.1016/j.jconrel.2021.09.033
Received 2 July 2021; Received in revised form 23 September 2021; Accepted 24 September 2021
Available online 27 September 2021

and increasing expression of PD-L1.

Physiologically, the STING pathway is activated by the binding of a specific ligand to the STING protein located at the endoplasmic reticulum (ER) [9]. Cyclic GMP-AMP (cGAMP) is a negatively charged cyclic dinucleotide (CDN), produced in the cytosol by cyclic GMP–AMP synthase (cGAS) in the presence of cytosolic dsDNA upon infection by an intracellular pathogen or in cancer cells. cGAMP is responsible for the activation of STING and downstream transcriptional factor leading to type I IFN production. Up to now, there are many cGAMP mimics synthesized that may serve as STING activators in cancer therapy [10]. To enable successful delivery of such cGAMP compounds to APCs, several important factors have to be taken into consideration. First, cGAMP is a dinucleotide prone to enzymatic degradation within the bloodstream. STING ligands therefore require protection by a suitable carrier, or chemical modification to confer higher enzymatic stability [11]. Secondly, as the target location for cGAMP is located within the cytosol of APCs, cGAMP has to cross the cell membrane, which is made of phospholipids, which are negatively charged just as cGAMP, hindering cell uptake. Therefore, there are three different possibilities: 1. intra-tumoral (i.t.) injection of soluble cGAMP, to achieve more localized delivery compared to 2. i.v. injection, for which in addition higher doses would be needed. Formulation of suitable delivery vectors, which will confer protection against degradation and provide efficient transfection of cGAMP, or 3. Synthetic modification of cGAMP or synthesis of its mimics.

In this review we will focus on the formulation of carriers for the successful delivery of cGAMP as it both enables its targeted delivery and protection against degradation and elimination. In order for the vectors to reach the APCs, many physicochemical characteristics that affect internalization and release of the cGAMP and eventual activation of the STING pathway need to be tailored [12–14]. In this review, we present different classes and types of carriers intended for cGAMP delivery, discuss their properties related to cGAMP delivery and their influence on successful STING pathway activation.

1.1. Mechanism of STING pathway activation

The cyclic dinucleotide (CDN) second messenger, cyclic GMP-AMP (cGAMP), is generated by cyclic GMP–AMP synthase (cGAS) upon detection of the presence of cytosolic dsDNA (either microbial or tumor DNA). cGAMP subsequently activates the pathway by binding to STING located in the endoplasmic reticulum (ER) [9] [4,15–18], which leads to its dimerization. After dimer formation, STING is translocated to perinuclear microsomes of the Golgi complex [19]. Downstream signaling includes the recruitment and activation (phosphorylation) of TANK-binding kinase 1 (TBK1), which in turn catalyzes the phosphorylation of regulatory transcription factor 3 (IRF3). IRF3 will translocate into the nucleus and will eventually upregulate the expression of type I IFN [20]. To a lesser extent, STING can activate the nuclear factor kappa-light-chain-enhancer of activated B cells (NF-κB) pathway, which in coordination with the TBK1-IRF3 pathway may induce the expression of type I IFN (Fig. 1) [1,19,21]. Upregulation of type I IFN results in maturation, migration, and activation of DC, T cells, and natural killer cells (NK) [15].

1.2. Role of STING pathway in different cells

The STING pathway can be activated in immune as well as tumor cells, where it was shown to directly activate senescence and apoptosis [22–24]. Moreover, initiation of apoptosis was also observed in T cells [25,26]. These findings are in contrast to the ones observed in DC, macrophages and mouse embryonic fibroblasts (MEFs), which are mostly apoptosis-resistant [25]. Among immune cells, DC though only representing 1% of total mononuclear cells, are the most important ones for STING activation and initiation of anti-tumor immunity [27]. It was shown that DC are 100 times more potent in initiation of an adaptive

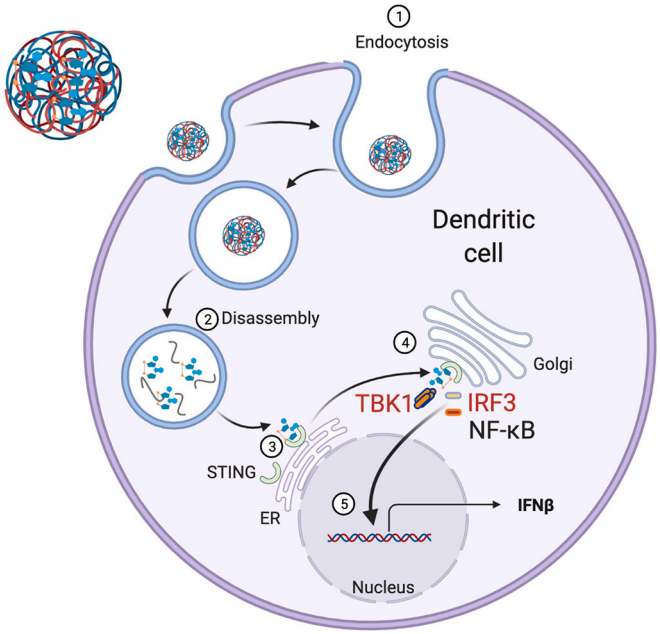

Fig. 1. STING pathway activation within dendritic cells.

immune response than monocytes and macrophages [27]. As described above, once located within DC, tumor dsDNA activates the STING pathway, leading to the production of type I IFN that enhances the cross-presentation of DCs by advertising antigen retention and CD8α + DC survival [28]. Once DCs are activated, they pass through phases of differentiation, maturation and upregulation of MHC-I, expression of CD40, CD80, CD86 and CD83 molecules, which in turn causes remarkable CD8+ T-cell responses [29,30]. In addition, type I IFN increases the expression of chemokines (CXCL9 and CXCL10), which is important for trafficking of effector T cells [31].

Moreover, cGAMP activates the STING pathway, which attracts macrophages into the tumor microenvironment. There are two macrophage phenotypes which are different in their activation and effector roles, M1 or classically and M2 or alternatively activated macrophages. M1 are supposed to exert antitumor activity, while M2 are immunosuppressive. The STING pathway in macrophages is activated by NF-κβ and IRF3 followed by production of type I IFN within M1 cells, while another transcriptional factor, STAT6, is activated within M2 cells, possibly being responsible for this polarization. [32]. The impact of STING on the polarization into these two macrophage types will be discussed in this review [6,33–35].

Gilliet et al. observed that besides DC, which are the main source of type I IFN, endothelial cells of the tumor microenvironment are involved in its production as well, suggesting a key role of the tumor vasculature in shaping the CD8+ T cell response [36]. Overall, the main target cells for STING pathway activation are APC and tumor cells, which will be discussed more in detail in this review.

1.3. STING pathway influence on tumor microenvironment

The tumor microenvironment (TME) consists of tumor cells, antigen-presenting cells (DC, macrophages), lymphocytes (T, B and NK cells) and fibroblasts. According to the degree of immune infiltration and possible inflammation, and eventual responsiveness to immune therapy, the TME can be classified into three groups: 1) “cold” or infiltrated – excluded (I-E) poorly immunogenic tumors; characterized by margins around the tumor mass where tumor-associated macrophages (TAM, often called M2 macrophages) prevent cytotoxic lymphocyte (CTL) infiltration into the tumor [8,37]; 2) “hot” infiltrated-inflamed (I-I) tumors; characterized by high CTL infiltration expressing immune checkpoint receptor

PD-1, and tumor cells expressing PD-L1 [8]; 3) TME-TLS, a subclass of inflamed tumors (I-I); histologically characterized by the presence of tertiary lymphoid structures (TLS), whose cellular composition is similar to lymph nodes consisting of lymphocytes (naïve and activated T cells), regulatory T cells (T_{reg}), B cells and DC [38,39]. As STING ligands promote the infiltration of T cells into the tumor (probably as a result of chemokines CXCL9 and CXCL10 production), and possibly impact on macrophage polarization, there would be space to explore whether STING ligands can switch the TME from "cold" to "hot" (I-E to I-I) [5, 33,41,42].

1.4. STING ligands

To provide external activation of the STING pathway, there was a need to extract eukaryotic/prokaryotic STING ligands or to synthesize enzyme-resistant mimics. The very first STING agonist DMXAA (also known as Vadimezan or ASA404) (Fig. 2 h) induced strong anti-tumor immunity and showed significant effect on tumor growth in mice, but it failed to improve frontline efficacy in advanced non-small cell lung cancer (NSCLC) in a phase III clinical trial, as it does not bind to human STING [43–46]. Motivated by the effect DMXAA had on tumors in mice, scientists attempted to identify more endogenous CDNs showing STING affinity. They showed that naturally occurring eukaryotic CDN 2′3′-cGAMP (Fig. 2 a) had higher affinity for STING and initiated stronger type I IFN responses compared to prokaryotic 3′3′-cGAMP (Fig. 2 b) and other CDNs (Fig. 2 c,d). For a more robust immune response and improved stability against enzymatic degradation, synthetic CDNs were developed apart from the natural ones [47–49]. CDA ML RR-S2 (Fig. 2e), also known as ADU-S100, developed by Aduro Biotech, is a synthetic STING ligand being more resistant than 2′3′ cGAMP to degradation by the major 2′3′-cGAMP hydrolase ectonucleotide pyrophosphatase (ENPP1), prolonging its systemic half-life [11]. ML RR-S2 also showed higher affinity for STING, improving IFN-β responses and tumor regression in established B16 tumors when compared to 2′3′cGAMP [44].

In contrast to the first generation of CDN-based STING agonists, limited to i.t. administration, non-nucleotide-based STING ligands were recently synthesized. Among them are SR-717 (Fig. 2f) intended for systemic administration and MSA-2 (Fig. 2 g), which is orally available in mice [49,50].

1.5. Combination therapies

As the response to immune checkpoint blockade (ICB; anti-PD-1/PD-L1 and anti-CTLA-4) therapy depends on tumor immune infiltrates, the combination with STING ligands would be beneficial for cancer treatment, especially as activation of the STING pathway leads to an increase in the expression of PD-L1 by tumor cells [51].

Currently, two phase I and one phase II clinical trials exploring the safety and efficacy of ADU-S100 (CDA ML RR-S2) in combination with immune therapy are ongoing:

- Phase I: Safety and efficacy of MIW815 (ADU-S100) +/− ipilimumab (anti CTLA-4) in patients with advanced/metastatic solid tumors or lymphomas (NCT02675439);
- Phase Ib: Safety and efficacy of MIW815 (ADU-S100) in combination with spartalizumab (anti PD-1)(PDR001) in patients with advanced/metastatic solid tumors or lymphomas (NCT03172936);
- Phase II: Efficacy and safety trial of ADU-S100 and pembrolizumab (anti PD-1) in head and neck cancer (NCT03937141).

Activation of dendritic cells within TME occurs once there is a sufficient level of tumor-associated antigens (TAAs) present. In order to reach the necessary antigen level, there is a need for their release from the cell, which occurs following tumor cell necrosis. In order to cause tumor necrosis and TAAs release, many treatments such as radiation or classical chemotherapy can be administered. Therefore, there is a rationale for the combination of some of the mentioned therapies with the activation of the STING pathway, resulting in synergic activation of dendritic cells [52].

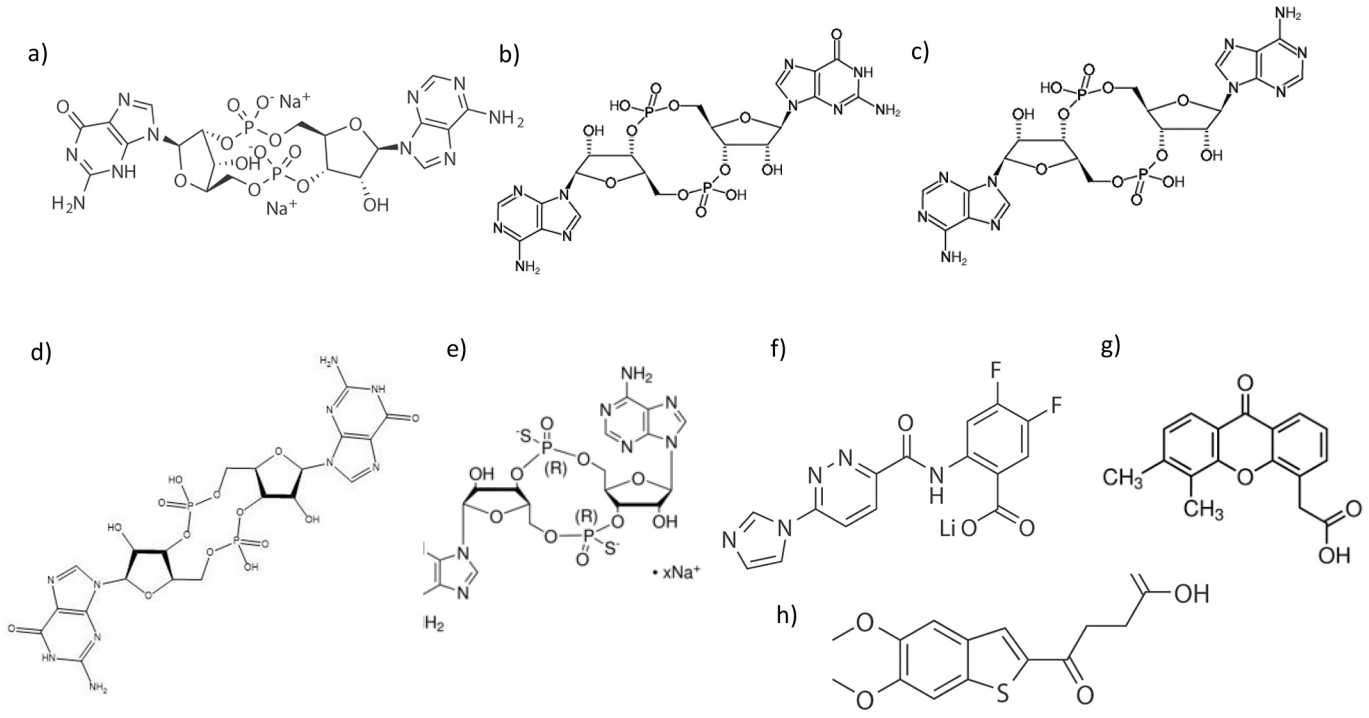

Fig. 2. Chemical structure of STING ligands: nucleotide – a) 2′3′-cGAMP b) 3′3′-cGAMP c) Cyclic di-AMP d) Cyclic di-GMP e) ML RR-S2 CDA; non nucleotide f) SR-717 g) DMXAA h) MSA-2.

1.6. Physicochemical properties of the carrier particles

Apart from possible degradation by different hydrolases, cGAMP possess physicochemical characteristics such as good aqueous solubility and negative charge, which are obstacles to cell membrane permeation. The ideal carrier should thus protect cGAMP from degradation and enhance its uptake. As for the latter, several parameters such as particle size and size distribution, shape, surface charge, surface functional groups and particle hydrophilicity should be taken into account (Table 1). The suitable particle size also depends on the route of administration. Upon systemic i.v. administration, several critical steps have to take place: avoiding clearance by the reticuloendothelial system (RES) and renal/hepatic elimination, permeation of the leaky tumor vasculature, and finally targeting TME [53]. A lower size limit to avoid renal clearance would correspond to the renal fenestration cutoff of around 5 nm, but the actual lower limit would be 50 nm, as smaller particles will interact with hepatocytes [54]. The upper limit varies from 400 to 600 nm to microns depending on the tumor epithelial fenestration [55]. These size limits are less stringent in case of i.t. injection, for which tumor penetration and cell uptake by antigen presenting cells are critical steps. Particles are internalized by APC via endocytosis, which can occur via two different pathways depending on the particle size and presence of receptor-mediated recognition: 1) phagocytosis (APC specific) or 2) pinocytosis (Fig. 3) [13,53,56].

Particle shape, whether spherical, ellipsoid or elongated can affect uptake, as well. It was shown that spherical particles are phagocytosed faster than those of ellipsoid shape, while worm/filament-like structures exhibited reduced uptake and showed a persistent circulation within the bloodstream [57,58].

Both positive and negative surface charges were favoring cell uptake compared to less charged or uncharged particles [14,53]. Specifically, functionalization with amine or carboxyl groups increased the cell uptake rate. In general, with an increase in hydrophilicity, uptake decreases. In addition, for some delivery vectors, a steric layer covering the particle surface is formed by PEGylation, which delays particle opsonization. As a result, phagocytosis as well as receptor-mediated uptake is delayed [14,59].

To enhance recognition and phagocytosis by DCs and avoid uptake by another cell type, carriers can be modified in order to target several DC receptors. The most prominent receptors expressed by DCs are the C-type lectin family members (DEC205 and mannose receptor), which are recognizing glycosylated antigens. Both DCs and macrophages express Fc receptors (FcRs) for IgE and IgG, eventually eliminating neutralized antigens through phagocytosis, may also be exploited for targeting of DC [27,60].

1.6.1. pH-responsive particles

Due to accumulation of lactic acid caused by anaerobic glycolysis, pH values within TME range from 6.5–6.9 [61]. In addition, intracellular compartments such as early endosomes, late endosomes, and lysosomes show pH values ranging from 6.5–4.5 [62,63]. Those different conditions can be exploited by formulating pH-triggered carrier systems able to respond to subtle pH changes, allowing for a successful drug "escape" from endosomes, while simultaneously protecting cGAMP from degradation. Besides different mechanisms of particle uptake, it was shown that only clathrin- mediated endocytosis leads to endosomal/lysosomal uptake and eventual release of the drug through above mentioned pH-triggered mechanism [13,14,64] (Fig. 3).

Once the particles reach the endosomal/lysosomal compartment there are two possible mechanisms of action concerning pH-sensitive particles. Carrier properties will change by protonation of either amino or carboxyl groups. This is especially important for amino groups, which will become positively charged within *endo*-lysosomes, causing the osmotic influx of water, resulting in lysosomal membrane rupture and finally drug release through a phenomenon called the "proton sponge effect" [63]. The other mechanism is based on carriers having groups cleavable at low pH such as amide, ester, imine, oxime, acetal or ketal functions. This is especially important for PEGylated particles where PEG is attached to the carrier through acid-labile linkers enabling drug release once those bonds are cleaved [65,66].

2. Polymers

Polymers are of interest in the field of non-viral genetic material delivery. They are relatively easily modified in terms of their chemical composition, molecular weight or molecular architecture. They protect the genetic material and provide controlled and targeted delivery [59,87]. Cationic polymers may benefit from ionic interactions to incorporate anionic cGAMP. Mostly used are synthetic polymers such as poly(L-lysine), poly(L-ornithine), linear and branched polyethyleneimine, diethylaminoethyl-dextran, poly(amidoamine) dendrimers, and poly(dimethylaminoethyl methacrylate) [88]. Natural polymers such as chitosan and its derivatives, dextran, and gelatin were also investigated for oligonucleotide delivery.

2.1. Biodegradable polymers

Watkins-Schulz et al. formulated particles using 70 kDa 40% acetylated dextran (Ace-DEX), a water-insoluble dextran derivative, which allows for the formation of stable microparticles that are hydrolytically cleaved in vivo into dextran, a Food and Drug Administration (FDA)-approved polysaccharide [72]. Particles were loaded with STING ligand 3′3'-cGAMP. A high loading capacity of 10.6 μg STING ligand per mg dextran at an encapsulation efficiency of close to 100% was achieved by fabricating particles by electro-hydrodynamic spraying. This biodegradable polymer has specific properties such as acid-sensitive degradation in lysosomes (pH = 5.0) and possible phagocytosis (Fig. 3) by antigen-presenting cells as target cells due to their size (nanoparticles loaded with STING ligand were around 700–1100 nm in size) [14,89,90]. As was previously reported, high STING ligand doses can cause T cell apoptosis [25,26]. The aim of this study was therefore to deliver the minimal possible dose of STING ligand (0.1, 1 and 10 μg tested), which can efficiently activate antigen-presenting cells using the most convenient route of administration out of four tested (i.v.; i.t.; i.p; i.m.). Ace-DEX MPs enhanced STING activation both in vitro and in vivo in two murine tumor models, the fast growing B16F10 melanoma and the slower growing triple-negative breast cancer (TNBC) model. Significant efficacy (cGAMP microparticles vs free cGAMP $p < 0.0001$) was proven at the lowest concentration reported up to now (0.1 μg), choosing the i.t. route of administration for further investigation. Additionally, at 10 μg i.t. administration of microparticles loaded with cGAMP, tumor survival was significantly higher ($p < 0.01$) compared to both PBS and vehicle. It was shown that NK cells were main participants of the immune response against fast growing tumors, while both NK cells and CD8+ T cells were responsible for the slower growing ones, probably as the adaptive immune response takes days to weeks to develop [2,72,91].

One of the polymers widely used in targeted and controlled delivery of therapeutic agents is polylactic-*co*-glycolic acid (PLGA). PLGA is a synthetic biodegradable polyester whose degradation occurs by hydrolysis of the polymer to lactic acid and glycolic acid. Depending on the ratio of these acids, release can be intended for long-term controlled drug release as for high lactide containing PLGA, while PLGA with lower lactide contents undergoes faster degradation. Polymer molecular weight also plays an important role in different release properties, where higher molecular weight would cause slower degradation due to the longer polymer chains [92]. In their work, Lu et al. developed a platform (cGAMP-MPs) suitable for controlled release over time in order to avoid multiple i.t. injections [73]. Especially in the case of hard-to-reach tumors where, in addition to side effects of injection, financial cost would be a limitation, as multiple image-guided injections would be required. Therefore, the aim of this work was to show that a single i.t. injection of

Table 1
Carriers for STING ligand delivery: CDG cyclic dimeric guanosine monophosphate; ML-RR-CDA - Dithio-(Rp, Rp)-2′,5′-3′,5′-c-diAMP sodium salt; DC-dendritic cells; M-macrophages; APC antigen presenting cells (both DC and M); TME –tumor microenvironment (immune+tumor cells); TC-tumor cells; nn non-significant; unk - unknown.

	Formulation	Carrier	Size (nm)	STING ligand	Tumor model	n0 tumor cells	Route of adm.	Dose (μg)	Total dose (μg)	Target cells	Tumor survival	*p* value	Ref
POLYMERS	Endosomolytic polymersomes	Poly(ethylene glycol)-*block*-[(2-diethylaminoethyl methacrylate)-*co*-(butyl methacrylate)-co-(pyridyl disulfide ethyl methacrylate)])	80	2′3′ cGAMP	E0771 breast cancer	5×10^5	i.v.	3 × 10	30	TME	cGAMP-particles vs vehicle	****	[67–69]
											cGAMP-particles vs free cGAMP	****	
	STING-NVs	PLA-b-PEG core and cytosine C rich i-motif DNA on the surface	45–117	cyclic di GMP	B16F10 melanoma	3×10^5	i.t.	5 × 3	15	APC	cGAMP-particles vs vehicle	ns	[70]
											cGAMP-particles vs free cGAMP	ns	
	PβAE/STING	Cationic and poly(beta-amino ester) (PβAE 447)	300	CDA ML RR-S2	B16F10 melanoma	2×10^5	i.t.	4 × 2	8	APC	cGAMP-particles vs vehicle	****	[71
											cGAMP-particles vs free cGAMP	****	
	Ace-DEX	40% acetalated dextran	687–1120	3′3’-cGAMP	B16F10 melanoma	2×10^5	i.t.	3 × 10	030	APC	cGAMP-particles vs vehicle	*****	[72]
											cGAMP-particles vs free cGAMP	ns	
	PLGA/STING	Polylactic-*co*-glycolic acid (PLGA)	4000x4000x3000	3′3’-cGAMP	B16F10 melanoma	2×10^5	i.t.	1 × 30	30	TME	cGAMP-particles vs vehicle	ns	[73]
											cGAMP-particles vs free cGAMP	ns	
	Mn-cGAMP NVs	Polymerized guanidine-containing disulfides (Gu + unit) to assemble with cGAMP and Mn2+ ion	168	2′3′ cGAMP	B16F10 melanoma	2×10^4	i.t.	3 × 1	3	DC	cGAMP-particles vs vehicle	ns	[74]
											cGAMP-particles vs free cGAMP	ns	
INORGANIC	CSiNPs	Cationic silica nanoparticles	35	cyclic di GMP	B16F10 melanoma	5×10^5	i.t.	1 × 5	5	TME	cGAMP-particles vs vehicle	ns	[75]
											cGAMP-particles vs free cGAMP	ns	
LIPOSOMES	Liposomal CGAMP-NPs	soy-PC/DOTAP	58–112	3′3’-cGAMP	C3 (1) Tag tumor	5×10^5	i.v.	7 × 10	70	M	cGAMP-particles vs vehicle	*	[76]
											cGAMP-particles vs free cGAMP	ns	
	PEG Liposome/ STING	DOTAP/cholesterol formulations with 0, 5, and 10 mol% PEG	160	2′3′cGAMP	B16F10 melanoma	2×10^5	i.t i.v.	4 × 1	4	DC	cGAMP-particles vs vehicle	unk	[77]

(*continued on next page*)

Table 1 (*continued*)

	Formulation	Carrier	Size (nm)	STING ligand	Tumor model	n0 tumor cells	Route of adm.	Dose (μg)	Total dose (μg)	Target cells	Tumor survival	*p* value	Ref
											cGAMP-particles vs free cGAMP	unk	
	PEGylated Liposome/STING	PEGylated liposomal carriers out of DOPC, DOPG, DMPC, DSPE-PEG	150	3′3′cGAMP	B16F10 melanoma	2.5×10^5	s.c.	1×5	5	APC	cGAMP-particles vs vehicle	****	[78]
											cGAMP-particles vs free cGAMP	****	
	pH-sensitive liposome	YSK05/POPE/cholesterol/DMG-PEG2000	150–200	cyclic di GMP	B16F10 melanoma	2×10^4	i.v.	3×1	3	M	cGAMP-particles vs vehicle	unk	[79,80]
											cGAMP-particles vs free cGAMP	unk	
	93-O17S-F/cGAMP	Lipid: head amine and acrylate (molar ratio 1:2.4). Lipid was mixed with cholesterol, DOPE, and C16-PEG2000-Ceramide (Avanti Polar Lipids) at a wt/wt ratio of 16:4:1:1.	114–170	2′3′cGAMP	B16F10 melanoma	5×10^5	i.t.	2×20	40	APC	cGAMP-particles vs vehicle	ns	[81–83]
											cGAMP-particles vs free cGAMP	ns	
HYDROGELS	STINGel	Positively charged peptide hydrogel - MultiDomain Peptide (MDP)	Bulk gel	CDA ML RR-S2	MOC2-E6E7 Head and Neck Squamous Cell Carcinoma	3×10^4	i.t.	1×20	20	TC	cGAMP-particles vs vehicle	*	[84]
											cGAMP-particles vs free cGAMP	*	
	STINGblade	Thermoresponsive hydrogel composed of laminin and collagen IV	Bulk gel	cyclic-di-AMP and rr-cyclic-di-AMP	SCCVII	5×10^5	i.t.	1×25	25	TME	cGAMP-particles vs vehicle	unk	[85]
											cGAMP-particles vs free cGAMP	unk	
	STING/HA	Scaffold by cross-linking hyaluronic acid	Bulk gel	2′3′-cGAMP	4T1 breast cancer invasive	1×10^5	i.t.	1×100	100	TME	cGAMP-particles vs vehicle	**	[86]
											cGAMP-particles vs free cGAMP	*	

* $p < 0.05$.
** $p < 0.01$.
*** $p < 0.001$.
**** $p < 0.0001$.

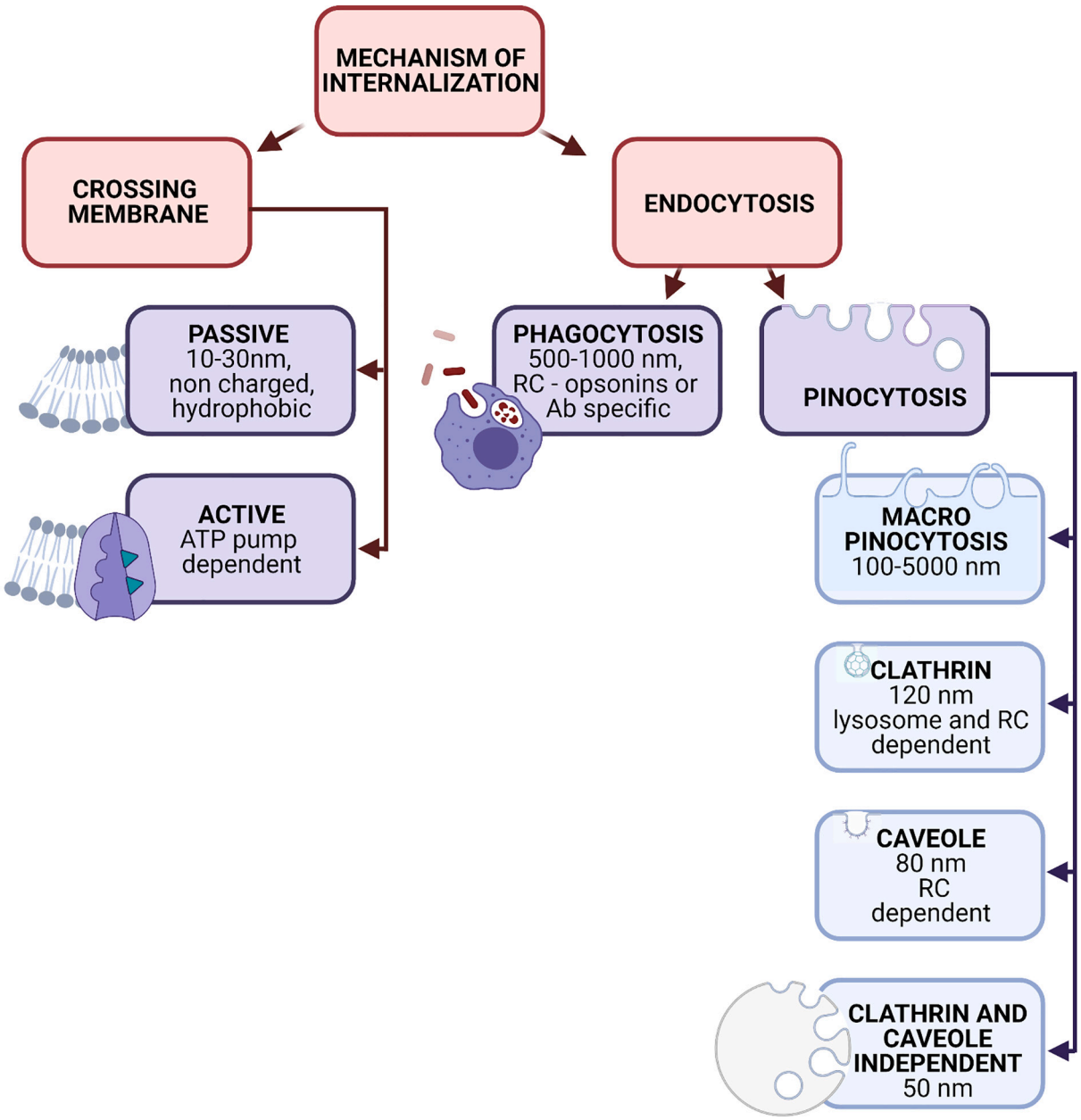

Fig. 3. Particle size influence on the internalization mechanism, independently of administration route. RC dependent – needs recognition by specific receptor to be taken up by cell. RC – receptor, Ab – Antibody. [13,14,27].

cGAMP-MPs would result in comparable or superior results in terms of tumor growth inhibition and survival as repetitive independent injections of soluble cGAMP . Particle formulation was done by a combination of several different techniques such as photolithography, soft lithography and ultralow-volume dispensing technologies where particles with square shaped dimensions (400 μm by 400 μm by 300 μm) were loaded with 2 μg of 3′3′ cGAMP. They physically mixed in a single injection different release profiles of PLGA-MP loaded with STING ligand. In their study they tested for in vitro/in vivo release using PLGA of different molecular weights (PLGA1 50:50, Mw 8.4 kDa, PLGA2 50:50 16 kDa, and PLGA3 60:40, Mw 22.2). As expected, based on their physicochemical properties release profiles were observed lasting between 4 ± 0, 8 ± 0 and 11 ± 1 days, respectively. There was no significant difference in antitumor efficacy of single-dose cGAMP-MP when compared to multiple injections of soluble cGAMP in several different animal models such as primary tumor (mouse B16F10 melanoma), effect on distant tumors (contralateral B16F0 melanoma), metastasis in the lungs (4 T1 breast cancer), orthotropic pancreatic cancer, and incomplete surgical removal tumor models. Additionally, cGAMP-MPs induced an immunogenic TME, showing infiltrating CD8+ T, NK and dendritic cells. Importantly, they also showed a shift from the alternative (M2) to the classical (M1) macrophage phenotype. Nevertheless, it was shown that infiltration of NK cells within the TME was significantly higher in case of three injections of soluble cGAMP compared to one time shot by cGAMP-MPs ($p < 0.01$) [73]. As previously described by Ting et al. where it was shown that NK cells were the main factors contributing to the arrest of tumor growth (same tumor model - B16F10 melanoma), it might be that more recurrent injections, or faster release is a promising strategy for effective cGAMP therapy.

2.2. pH-sensitive polymers

Nanocarriers sensitive to pH changes may benefit from a facilitated lysosomal escape, as illustrated by several literature reports [93–95]. In

order to formulate a cancer vaccine based on nanotechnology ("nanovaccine"), which will target secondary lymphoid organs, suitable for endosomal escape of the drug and eventually initiating robust tumor-specific T cell response, Luo et al. performed a screening of a library of ultra-pH sensitive (UPS) nanoparticles (20–50 nm in diameter). These micellar NPs are based on PEG-co-pentamethyldiethylenetriamine containing tertiary amines with linear or cyclic side chains [62]. It was previously reported that particles smaller than 50 nm can selectively accumulate in secondary lymphoid organs, targeting APC; however, not all of them can boost the immune response in the absence of incorporated adjuvants [62,96,97]. Nevertheless, PC7A NP was the best candidate based on ovalbumin (OVA)-specific CTL responses [95]. PCA7 (PEG-*b*-poly(2-(hexamethyleneimino)ethyl methacrylate) block copolymers were synthesized by atom transfer radical polymerization. It was demonstrated that the platform together with the STING ligand 2′3′-cGAMP provided efficient antigen delivery and cross-presentation, boosting antitumor immunity. In addition, tumor growth was lower for CpG loaded in OVA nanovaccine compared to OVA soluble CpG ($p < 0.01$) in a melanoma tumor model, with no difference in survival. Moreover, their nanovaccine in combination with an anti-PD-1 antibody resulted in 100% survival over 60 days in a murine TC-1 tumor model [95]. In their further work, they combined PC7A NP with radiation therapy, which causes tumor DNA leakage into the cytoplasm, eventually activating the STING pathway [29]. By damaging tumor cells, radiation causes the release of TAAs and increased activation by dendritic cells (radiation+particles vs particles $p < 0.01$) [52]. In combination with STING ligand, they showed antitumor efficacy in both large, established solid tumors as well as in distal tumors [98]. Taken together, these data suggest the importance in synergizing STING activation with radiation therapy for a successful antitumor efficacy.

Similar to PC7A NP, Wilson et al. developed a pH-responsive platform named endosomolytic polymersomes [67]. The polymersomes consist of an aqueous core for STING ligand 2′3′cGAMP loading surrounded by a vesicle membrane made of block copolymers poly (ethylene glycol)-*b*-[(2-diethylaminoethyl methacrylate)-*co*-(butyl methacrylate)-*co*-(pyridyl disulfide ethyl methacrylate)]) (PEG-*b*-DB), enabling STING ligand encapsulation efficiency of about 38%. PEG–*b*-DB features a polycarbonate backbone with side-chain amines, which promote the disassembly of nanoparticles in response to pH conditions (5.5–4.5, from early endosome to lysosome) [99]. Once polymersomes were formulated and loaded with STING ligand, polymer chains were cross-linked in situ by disulfide bridges. Polymersomes maintained the ability of pH-responsive disassembly after crosslinking, as confirmed by a decrease in nanoparticle size (to below 80 nm) at endosomal pH. This platform enhanced STING ligand activity by 240- to 610-fold in THP-1 ISG, RAW ISG, and B16 ISG cell lines. The increased potency was achieved by enhanced endosomal escape and cytosolic delivery of the STING ligand. Moreover, it was shown that macrophage and DC cell lines are more prone to the uptake of polymersomes (RAW ISG > DC2.4 > NK > B16.F10). Administered locally in the murine melanoma model, a decrease of CD206, a marker of M2-polarized macrophages, was shown. In addition, a significant increase in the number of infiltrating CD8+ and CD4+ T cells within the TME was observed, suggesting a switch from "cold" to "hot" tumors [5]. I.t. administration (10 μg of STING ligand per injection) decreased tumor growth rates by eleven-fold (cGAMP particles vs free cGAMP $p < 0.05$), and prolonged survival significantly (cGAMP particles vs both free cGAMP and free vehicle $p < 0.0001$). Moreover, the therapeutic efficacy was achieved in combination of i.t. polymersomes with intravenous injection of anti-PD-1 and anti-CTLA4 ICB. Altogether, it was shown that polymersomes were able to successfully deliver a STING ligand into the cytosol of antigen-presenting cells, switching TME immune status by immune cell infiltration and macrophage repolarization [67]. In their further work, Wehbe et al. used a polymersome platform for 2′3′ cGAMP in order to improve cGAMP half-life after i.v. administration. This platform not only increased half life of cGAMP by 40-fold, resulting in cGAMP accumulation within TME, but also drastically increased tumor-infiltrating T cells in several tumor models (melanoma B16-F10, breast cancer models E0771 and YUMM1.7, $p = 0.0015$). In addition, both tumor growth inhibition and survival were significantly improved with polymersomes compared to soluble cGAMP ($p < 0.0001$). Up to now, this is a first work connecting PK and PD of a STING-activating nanomedicine, offering the option of i.v. administration [68]. Moreover, to scale up the process, Nguyen et al. changed synthesis to avoid additional cGAMP purification process, by selecting PEG–*b*-DB for PEG-functionalized methacrylate (PEGMA), which was later copolymerized with DEAMEA and BMA, resulting in their final formulation PEGMA-*co*-DEAEMA-*co*-BMA graft copolymers. By varying the molecular weight of PEGMA monomers (300 and 950 Da) and the percentage of PEG (20, 25, 30 wt%), they discovered the connection between polymer structure, self-assembly properties, endosomal escape and cGAMP activity, using 300 Da PEGMA with both 20 and 25% PEG for the strongest STING activation [69].

Another pH-responsive polymer used as a carrier for cancer therapy was reported by Zhang et al., consisting of a PLA-b-PEG core and cytosine C rich i-motif DNA on the surface [70]. I-motifs are DNA with multiple domains of consecutive cytosines in each C domain. At physiological pH those motifs are linear, while at low pH they form so-called C-quadruplexes via C:C+ base pairing. To build their STING nanovaccine (STING-NV), the STING ligand cyclic dimeric guanosine monophosphate (CDG) was loaded into i-motif DNA at physiological pH. Guanosine (G) from CDG and the cytosine present in i-motifs were interacting through hydrogen bonding. They confirmed the hypothesis that the release of the drug would be triggered by a lower pH (corresponding to the endosomal pH) through conformational changes of i-motifs, which would switch from linear strands to C-quadruplexes. With a loading efficiency of 53 ± 1%, a size of 81 ± 36 nm, successful endosomal escape of CDG and 55–65% release within the cell, at a dose of 3 μg every 3 days over 15 days, STING-NVs antitumor efficacy (tumor growth) was significantly improved compared to blank particles (5C-i-motif-modified NPs (5C-NPs) (cGAMP particles vs blank $p < 0.0001$; cGAMP particles vs free cGAMP ns)) with the trend towards superior efficacy compared to CDG-loaded cationic liposomes (Lipo-CDG). Additionally, in both human and mouse immune cells (macrophage, DCs and monocytes) an increase in IFN type I secretion was observed. They also showed repolarization of macrophages from M2 to M1 and an increase of MHC II and CD86 markers characteristic for M1 and down-regulation of CD206 markers characteristic for M2 [70]. STING-NVs might be an effective platform for pH-sensitive STING ligand delivery in the poorly immunogenic melanoma model.

One limitation of STING ligands is their propensity for in vivo degradation. To address this issue, Wilson et al. designed modified STING ligands (ML-RR-CDA) of increased in vivo stability and enhanced human STING activation, and RR-CDG, a phosphodiesterase resistant version of cyclic-di-GMP [72]. Particles with modified STING ligands and poly (beta-amino ester) (PβAE 447) were prepared. Amino groups in PβAE allow for electrostatic interaction between the positively charged protonated amino groups of the polymer and the negatively charged phosphate groups of the STING ligand [100]. As already discussed in this review, positively charged particles are able to trigger endosomal escape of the drug through the "proton sponge effect" [66]. Nanoparticles were prepared at a 1:500 *w*/w ratio of PβAE/STING ligand in 150 mM PBS. The measured particle size differed between the different methods used, i.e. dynamic light scattering (DLS, around 300 nm), nanoparticle tracking analysis (NTA, around 100 nm) and transmission electron microscopy (TEM, around 80 nm). No significant difference in size was observed in the presence or absence of the STING ligand. Once lyophilized with sucrose as a cryoprotectant and stored at −20 °C, particles were able to exert a highly effective IRF3 activation for at least 9 months. Particles were administered i.t. in B16-F1 melanoma tumors in combination with intraperitoneal administration of anti-PD-1 (cGAMP 2μg + aPD1). This combination resulted in a statistically significant

reduction of tumor growth compared to the free STING ligands ($p < 0.0001$) [72].

Chen et al. speculated that cGAMP might be degraded in the acidic environment of the lysosomal compartment [74]. Therefore, they manufactured a platform called Mn-cGAMP NVs based on polymerized guanidine-containing disulfides and Mn^{2+}, having a size of around 160 nm (TEM 160 nm, DLS 168 nm ± 20 nm). Thiol-mediated endocytosis is a receptor-mediated mechanism avoiding the *endo*-lysosomal pathway. By exploiting this pathway for cGAMP delivery, lyso-endosomal degradation was avoided. Possible 2′3′CGAMP degradation was prevented by adding Mn^{2+}. Enhanced secretion of cytokines (IFN-β, IL-6, and TNF-α) by DC and CD8+ T cell recruitment within TME was demonstrated. Moreover, tumor growth was significantly lower compared to soluble cGAMP ($p < 0.0001$). In addition, improved survival was also observed for their system compared to soluble cGAMP.

Physicochemical properties such as size, shape, zeta potential, surface decoration of the particles serving as a delivery system for cGAMP are pivotal for successful transfection. Surface charge is an important parameter as previously explained. We can observe that, e.g., in the work of Shae et al. and Wilson et al. who used carriers displaying amino groups on their surface. Survival was significantly increased compared to soluble cGAMP, probably due to a proton sponge effect exerted and a release of cGAMP into the cytosol. Depending on the route of administration, the target particle size should be adjusted. Particles smaller than 50 nm applied i.v. would probably be extracted and degraded by the liver and/or excreted by the kidneys. In order to permeate the tumor (neo) vasculature and reach the tumor mass, particles should pass through endothelial fenestrations, which are 600 nm to a micron in size. Optimal size might be different when it comes to i.t. administration depending on the targeted cells. It appears that the bigger the particles, the more pronounced is their internalization by APC, probably due to phagocytosis (Fig. 3). Accordingly, Watkins-Schulz prepared particles of 687–1120 nm in size, using the lowest dose to date of 0.3 μg cGAMP, which showed a significant decrease in tumor growth compared to soluble cGAMP ($p < 0.0001$) [72]. Zeta potential and shape of particles may also be important to take into account but have not often been described in the reported work. One of the possibilities to enable not only successful internalization but also drug endosomal escape is the use of pH-responsive nanoparticles. For instance, endosomolytic polymersomes are vesicle sensitive to lower pH values and allow for endosomal cGAMP escape [67]. Besides the proton sponge effect for particles containing primary and secondary amino groups, with drug release due to osmotic endosome swelling and covalent bond cleavage, Zhang et al. discussed a drug release mechanism driven by conformational changes of i-motif DNA at lower pH values [70]. The pH-responsive feature can be a promising one, but in order to target the internalization by the *endo*-lysosomic pathway, it is important to take into account other parameters such as particle size enabling clathrin mediated endocytosis. On the other hand, Chen et al. formulated Mn-cGAMP NVs, which were taken up by thiol-mediated endocytosis and directly delivered to the cytosol, avoiding possible cGAMP degradation in the lysosomal compartment [74].

Frequent i.t. administration may damage vascular networks and cause metastasis. Therefore, particles or hydrogels able to release cGAMP in a sustained manner might be administered once and possibly cause lower damage. Lu et al. showed that by incorporating cGAMP in PLGA microcontainers/particles with different release properties resulted in a tumor growth control similar to 4 repeated administrations of soluble cGAMP [73]. With regards to tumor immunogenicity and microenvironment, melanoma, a poorly immunogenic tumor was one of the most examined tumors discussed here. Activation of the STING pathway is able to cause M2 phenotypic switching to M1 macrophages, increase T cell infiltration and increase PD-L1 receptor expression, which altogether can turn poorly immunogenic tumors such as melanoma to immune-infiltrated "hot" tumors. This attractive property was used in order to apply and combine anti-PD-L1 therapy, whose synergistic effect was clearly demonstrated by the work of Wilson et al. where particles made of cationic polymer PβAE and ML-RR-CDA in combination with anti PD-L1 administration significantly decreased tumor growth compared to soluble ML-RR-CDA ($p < 0.0001$) [71]. When it comes to solid tumors, such as cervical tumors, the release of the tumor antigens would be beneficial in order to activate APCs. Therefore, radiation therapy causing tumor necrosis and successive tumor antigen release was combined with cGAMP within PEG-co-pentamethyldiethylenetriamine carriers by Luo et al. This combination resulted in a synergistic effect, causing a significant decrease in tumor growth ($p < 0.001$) [98].

3. Inorganic particles

In their work, An et al. took advantage of the ability of inorganic particles to provoke intrinsic cytotoxicity to attack cancer cells, eventually causing their destruction [75]. Moreover, they combined cationic silica nanoparticles (CSiNPs) with negatively charged STING ligand *c*-di-GMP (200/1 mass ratio, size 35 nm, ZP +18 mV, encapsulation efficiency 65%) facilitating cellular uptake and significantly enhancing the number of antigen-specific CD8+ T cells within TME in murine melanoma. I.t. injection of CSiNPs (5 μg of STING ligand per injection) lead to acute cell necrosis disrupting the plasma membrane and inducing the production of reactive oxygen species (ROS) in TME. As particles were around 30 nm in size, one of the possible reasons of induced toxicity may be the size, as it was already reported that silica particles smaller than 50 nm can cause necrotic cell death in endothelial cells. Altogether, these data suggest that CSiNPs possibly may be a new in situ vaccine platform for local tumor destruction by immune activation. However, the contribution of the CSiNPs carrier alone to the inflammation has not been reported.

4. Liposomes

Liposomes are characterized by their often PEGylated phospholipid bilayers stabilized by cholesterol and resembling cell membrane structures. They are generally biocompatible and show low immunogenicity and toxicity, and by protecting the encapsulated active principle liposomes can increase therapeutic efficacy [101]. Liposomal formulations can be adjusted by altering the ratio between hydrophilic and hydrophobic parts of phospholipids, which will result in a better loading capacity of the drug depending on their physicochemical properties [102]. The hydrophilic head groups of lipids can be cationic, neutral or anionic. If primary or secondary amino groups are present in the structure of the hydrophilic head groups, liposomes can release the drug from the lysosome, allowing it to escape by virtue of the "proton sponge effect" [103,104]. The hydrophobic hydrocarbon chains and the hydrophilic ammonium or tertiary amine head are connected by either ester, amide or ether bonds. To confer pH-responsive delivery properties, these bonds can be modified into ortho-ester, carbamate or hydrazone bonds [105,106]. Altogether, cationic liposomes would be a suitable platform to load STING ligands by interacting with anionic phosphate groups, protecting their structure and eventually providing endosomal escape.

Cheng et al. formulated liposomes prepared from soy-PC/DOTAP (100/1 *w*/w) loaded with STING ligand 3′3'-cGAMP, resulting in particles of 85 nm, a zeta potential of +14 mV, and an EE of 40% [76]. The team focused on cancer types that have limited or no response to PD-L1–targeted treatments, or in general cancer immunotherapy [107–109]. In both melanoma and TNBC models, they showed that the therapeutic efficacy through tumor growth of their liposomal particles, fully depending on activation of the STING/IFNAR pathway, once administered intravenously was significantly higher using 60× lower dose (1μg/ml of STING ligand) compared to the free soluble drug reported in Corrales's work [44] and compared to the soluble cGAMP in their work (cGAMP particles vs free cGAMP $p < 0.05$). Moreover, particles caused increase in CD8+ cytotoxic T cells, preventing the

development of secondary tumors. Additionally, they performed experiments to check the dominant phenotype of macrophages (pro-tumoral M2-like or a tumor-suppressive M1-like) [7]. Results showed that both in vitro and in vivo, liposomal cGAMP-NPs polarized macrophages from M2-like to M1-like phenotype. Liposomes also enhanced M1-like markers (IL-6 and TNF and nitric oxygen species) and reduced M2-like markers in a genetically engineered mouse model of basal-like TNBC. This may suggest another example of a switch from "cold" to "hot" tumors [5,76].

Koshy et al. prepared cationic liposomes to improve the potency of STING ligands for cancer immunotherapy [77]. Three DOTAP/cholesterol formulations with 0, 5, and 10 mol% PEG were used and loaded with 2′3′cGAMP STING ligand. Size of the particles, either loaded with ligand or empty, was around 160 nm in PBS. In order to examine whether cationic particles were prone to aggregation and interaction with anionic serum proteins, size measurements in complete cell culture medium containing 10% fetal calf serum (FCS) were performed. Incorporation of 5 to 10 mol% of PEGylated phospholipids in the liposomal membrane prevented increase of the liposome diameter when suspended in complete cell culture medium, suggesting that PEGylation reduced protein binding and eventually potential aggregation [14,59,77]. Additionally, zeta potential was measured showing that PEGylation affected surface charge, decreasing its value in the formulations with higher density of PEG at the particle surface. Cell association and uptake by bone marrow dendritic cells (BMDC) was faster and liposomes were found to be more numerous in the cytoplasm in the case of non-PEGylated liposomes. The higher positive charge (around 40 mV) compared to PEGylated particles (around 20 mV) might be a reason of better and faster uptake [14]. In vivo testing was performed with the lowest PEGylation density, to ensure stability in serum. Nevertheless, once administered i.t. (1 μg of STING ligand) in a murine melanoma model, non-PEGylated liposomes were not efficient in tumor growth, resulting in incomplete tumor control. In contrast, treatment with 5, and 10 mol% PEGylated liposomes decreased tumor growth in 50% of the mice, in spite of the lower in vitro efficacy of the PEGylated liposomes (cGAMP PEG5 particles vs free cGAMP: ns; cGAMP PEG5 particles vs PBS: $p < 0.01$). Later on, groups were re-challenged with B16-F10 cells, showing high percentage of survival at 60 days (free drug 50%, PEG5 75%, PEG10 100%) (cGAMP PEG10 particles vs free cGAMP ns; cGAMP PEG10 particles vs PBS $p = 0.017$). Additionally, Intravenously injected PEG5-cGAMP lead to an increase in cytokine production (~200× and ~1400× increases in IFNB1 and CXCL9 expression, respectively) compared to soluble cGAMP and therefore increased therapeutic efficacy against metastatic melanoma in the lung [77].

Hanson et al. prepared PEGylated liposomal carriers using DOPC, DOPG, DMPC, DSPE-PEG/STING ligand 3′3′cGAMP, having a size of around 150 nm [78]. Once particles were administered subcutaneously (5 μg of STING ligand loaded), they showed enhanced STING pathway activation in APC and 15-fold increase in particle accumulation in lymph nodes compared to the free soluble drug (ns). Furthermore, an increase in adaptive immunity response (both humoral and cellular) to weakly immunogenic antigen at doses 30 times lower than for free STING ligand was observed. Moreover, survival was increased in ovalbumin (OVA) liposome formulation compared to OVA soluble cGAMP ($p < 0.0001$).

Nakamura et al. tested a pH-sensitive formulation (YSK05/POPE/Cholesterol 40/30/30 + STING ligand) as an adjuvant system for cancer immunotherapy, administering liposomes s.c. in preventive tumor models (0.1 and 0.3 μg of cyclic di-GMP STING ligand per mouse) [79,80]. YSK05 lipid was chosen as it contains long, unsaturated carbon chains and one tertiary amino group, responsible for its pH-sensitive fusogenic nature [110]. Particles were around 150–200 nm in size, and in both cases slightly negatively charged. Then, the formulation was changed (YSK05/POPE/cholesterol/DMG-PEG2000 40/25/35/1 + STING ligand) by PEGylation of the particles, and NK cell activation tested after i.v. administration in a metastatic melanoma model (3 μg of STING ligand/mouse). They could show high fusogenic and endosomal escape properties of YSK05 by measuring IFN-β. No effect on cytokine production in RAW264.7 cells (macrophages) without STING ligand was shown in spite of high uptake rates. Additionally, liposome vaccination augmented the expression of costimulatory molecules (CD80, CD86) and MHC class I, and showed higher CTL activities. Altogether, it was suggested that this platform in combination with STING ligand can serve as an adjuvant in vivo [79]. As mentioned above, in the second part of the work, an MHC-I non-restricted antitumor effect by NK cell activation by markers of NK cells, NKG2D and CD69 was observed to be significantly increased. Furthermore, tumor growth was significantly inhibited in mice compared with the control groups ($p < 0/01$) [80].

Due to immunosuppressive tumor microenvironment in melanoma, and poor TAA presentation to APC, in situ vaccination has had limiting efficacy. Therefore, Chen et al. first administered i.t. doxorubicin at day 0, in order to cause local necrosis and local TAA relesase, followed by day 1 administration of 93-O17S-F/cGAMP particles [81]. In order to formulate cationic synthetic LNPs able to complex negatively charged cGAMP and eventually release it by lyso-endosomal escape, Chen et al. screened the LNP library for delivering the model antigen OVA, and chose 93-O17S-F as it had the best IgG1 and IgG2c antibody response. 93-O17S-F is composed of a lipid, which is synthesized out of head amine and biodegradable acrylate featuring disulfide bond (molar ratio of 1:2.4) and mixed with cholesterol, DOPE, and C16-PEG2000-ceramide at a weight ratio of 16:4:1:1 [82]. Final particles had a size of 114–170 nm [83]. Significant increase in CD4+ T cells, CD8+ T cells, macrophages, phenotype switch from M2 to M1 was shown. Total tumor reduction was present only with the combination of DOX followed by 93-O17S-F/cGAMP (tumor volume was significantly lower in case of DOX 93-O17S-F/cGAMP compared to both 93-O17S-F/cGAMP and DOX-cGAMP administration ($p < 0.001$)).

Surface decoration, e.g., by PEGylation, is an important parameter for i.v. administration as hydrophobic particles may be more readily opsonized by the RES limiting their ability to reach the target site. Therefore, surface PEGylation can protect particles from premature cell uptake, at least transiently. Different percentage of PEG surface decoration resulted in different uptake rates with lower percentage of PEG increasing uptake by APCs as described in work of Hanson et al. [78]. As previously described, surface charge is another important parameter. Cationic liposomes using fusogenic YSK05 lipid with positively charged tertiary amino group were designed to exert proton sponge effect and eventual release of cGAMP in the work of Nakamura et al. [79,80]. In order to achieve the release of TAA and cross-present them to APC, Chen et al. [81] first administered i.t. doxorubicin and additionally their lipidoid nanoparticles 93-O17S-F loaded with cGAMP, showing that significant tumor reduction was possible only with doxorubicin pretreatment. That was another work besides radiation [98] showing that a combination of a delivery system containing cGAMP with the technique/medication causing release of TAA results in significant difference in tumor growth compared to no combination or soluble cGAMP.

5. Hydrogels

I.t. injection of STING ligands has been demonstrated to be efficacious in a range of tumor models and mouse backgrounds [111]. However, by this route of administration STING ligands can undergo a fast dissemination from the injection site into the systemic circulation [112]. Hence, hydrogels with tunable physical properties allowing for a release of the drug in a controlled and/or sustained fashion and to protect the drug from degradation is considered a powerful approach to achieve better therapeutic outcomes of STING ligands while limiting systemic toxicity [113].

Leach et al. developed the STINGel platform, consisting of a positively charged peptide hydrogel called MultiDomain Peptide (MDP), which is easily delivered through a syringe to TME, targeting cancer cells. MDP has been used for mixing and crosslinking with anionic

molecules such as CDA ML RR-S2, eventually leading to self-assembly forming a nanofibrous matrix [84]. STINGel loaded with 20 μg of STING ligand showed an 8-fold slower release rate compared to a STING ligand loaded into a collagen gel ($p < 0.0498$). In addition, the use of STINGel lead to a six-fold increase in survival in a challenging murine model of head and neck cancer when compared to collagen as a matrix. Moreover, compared to soluble cGAMP, STINGel improved mice survival significantly ($p < 0.282$).

Baird et al. formulated a STING-targeted surgical immunotherapy platform in the form of a thermoresponsive hydrogel composed of laminin and collagen IV of animal origin called STINGblade [85]. In preclinical models of head and neck squamous cell carcinoma (HNSCC), this hydrogel-like formulation of STING ligands is based on Matrigel®, which is a liquid when refrigerated and turns into a bulk gel following in vivo application. The obtained results following application in local TME treatment (cyclic-di-AMP and rr-cyclic-di-AMP, 25 μg per treatment) appeared to be entirely depending on host cell expression of STING and IFNAR1 and mediated by CD8+ T cells. Although STINGblade is effective locally, it does not have an impact on distant metastases. Even mice that had their primary tumor completely resolved by STINGblade did not experience improved overall survival, suggesting that local therapy was insufficient to effectively treat this distant disease in the 4 T1 model, a more aggressive model of lung metastases. Additionally, a tumor explant model was developed and treated ex vivo with STING ligands in tumors from both mice and patients. The analysis of the cytokine response consistently resulted in a statistically significant increase in IFNα and CCL3 secretion, while IFNβ, TNFα, and IL10 secretions tended to be more patient-specific, showing none of the patients with significant increase in CXCL10 secretion. These data might suggest possible personalization of cancer immunotherapy-containing biomaterials based on cytokine response to STING ligands in a tumor explant model [85].

Park et al. prepared a hydrogel scaffold by cross-linking hyaluronic acid in a mold. As surgery produces a transient immunosuppressive state leading to an increase in metastasis, the formulation was applied in multiple models of spontaneous metastasis [86]. A biodegradable hydrogel placed into the tumor resection site showed that local release of agonists of innate immunity such as TLR7/8 or STING ligand (dose: 100 μg of 2′3′-cGAMP) increased the number of activated NK cells, dendritic cells, and T cells and induced the production of large amounts of type I interferons preventing tumor recurrence, eliminating distal metastases and increasing tumor survival (cGAMP bulk gel vs free cGAMP $p < 0.05$; cGAMP bulk gel vs vehicle $p < 0.01$). Thus, TLR7/8 and STING ligand within the bulk gel serve as adjuvants at the tumor resection site, reprogramming an immunosuppressive environment into an immunostimulatory one and thereby stimulating systemic antitumor immunity curing a much higher percentage of animals than the systemic or local administration of the same therapy in solution [86].

Formulations being liquid at room temperature and gelling at 37 °C may be able to reach all tumor stroma before turning into bulk gels and therefore release cGAMP from inside and outside the whole tumor mass/volume might be promising approach. Such work was performed by Park et al., where STINGblade made of Matrigel loaded with cyclic-di-AMP and rr-cyclic-di-AMP significantly decreased tumor growth compared to empty particles ($p < 0.0001$) [86]. Synthetic substitutes to Matrigel®, a complex matrix of animal origin, may hold promise for intra-tumoral delivery, however, there is still a need of in vivo examination.

6. Summary and future perspectives

cGAMP has the potential to activate the STING pathway but requires a carrier to avoid enzymatic degradation in the blood and to reach the cytosol of APCs. When designing particles for successful cGAMP transfection, many parameters should be taken into account in order to achieve the maximum possible effect at the lowest dose possible, causing minimal unwanted side effects. Designing particles for i.v. cGAMP delivery remains a challenge, due to a potential premature uptake by the RES, and the possibility of a cytokine storm as a result of STING hyperactivation. Therefore, in clinical research i.t. is the only approved administration, even though limited to accessible lesions only. Although many carriers were designed for cGAMP delivery, none of them reached the clinical level. Based on the choice of the carrier there are possibilities for different release profiles of cGAMP. For instance hydrogels or sustained release polymers avoid repetitive i.t. administrations, which might induce metastasis. Another i.t. modality for hydrogels is the application after surgical resection tumor resection (Baird et al. and Park et al.), where cGAMP-loaded hydrogels may prevent tumor relapse.

In the search for intracellular delivery of STING ligand, nanocarriers demonstrated preclinical efficacy in several tumor models. As a perspective towards a better understanding of carrier properties, parameters such as zeta potential, shape of the particles and encapsulation efficiency must be determined and clearly documented. Size and charge of the particles play a role in different uptake and release mechanism, especially in the case of pH-responsive particles, where either charged polymers or liposomes caused significant decrease in tumor growth compared to soluble cGAMP. Moreover, the nature of the STING modulator-cGAMP, its dosage, encapsulation efficiency and the tumor type are also important parameters. Depending on the cGAMP used, results might be improved, as illustrated by molecules such as CDA ML RR-S2 or recently synthesized non-nucleotide STING modulators such as SR-717 and MSA-2 that are more resistant against enzymatic degradation. Combination with a pretreatment of the tumor allowing TAA release before administering particles loaded with cGAMP might be one of the perspectives for a successful clinical application.

References

[1] G.N. Barber, STING: infection, inflammation and cancer, Nat. Rev. Immunol. 15 (12) (2015) 760–770.
[2] T.F. Gajewski, H. Schreiber, Y.-X. Fu, Innate and adaptive immune cells in the tumor microenvironment, Nat. Immunol. 14 (10) (2013) 1014–1022.
[3] A. Li, et al., Activating cGAS-STING pathway for the optimal effect of cancer immunotherapy, J. Hematol. Oncol. 12 (1) (2019) 35.
[4] L. Corrales, et al., The host STING pathway at the interface of cancer and immunity, J. Clin. Invest. 126 (7) (2016) 2404–2411.
[5] M. Binnewies, et al., Understanding the tumor immune microenvironment (TIME) for effective therapy, Nat. Med. 24 (5) (2018) 541–550.
[6] J.A. Van Ginderachter, et al., Classical and alternative activation of mononuclear phagocytes: picking the best of both worlds for tumor promotion, Immunobiology 211 (6–8) (2006) 487–501.
[7] N. Wang, H. Liang, K. Zen, Molecular mechanisms that influence the macrophage m1-m2 polarization balance, Front. Immunol. 5 (2014), 614.
[8] S. Spranger, Mechanisms of tumor escape in the context of the T-cell-inflamed and the non-T-cell-inflamed tumor microenvironment, Int. Immunol. 28 (8) (2016) 383–391.
[9] H. Ishikawa, G.N. Barber, STING is an endoplasmic reticulum adaptor that facilitates innate immune signalling, Nature 455 (7213) (2008) 674–678.
[10] X. Cui, et al., STING modulators: predictive significance in drug discovery, Eur. J. Med. Chem. 182 (2019), 111591.
[11] L. Li, et al., Hydrolysis of 2′3′-cGAMP by ENPP1 and design of nonhydrolyzable analogs, Nat. Chem. Biol. 10 (12) (2014) 1043–1048.
[12] C. Foged, et al., Particle size and surface charge affect particle uptake by human dendritic cells in an in vitro model, Int. J. Pharm. 298 (2) (2005) 315–322.
[13] L.A. Mulcahy, R.C. Pink, D.R.F. Carter, Routes and mechanisms of extracellular vesicle uptake, J. Extracellular Vesicles 3 (2014), https://doi.org/10.3402/jev.v3.24641.
[14] K. Kettler, et al., Cellular uptake of nanoparticles as determined by particle properties, experimental conditions, and cell type, Environ. Toxicol. Chem. 33 (3) (2014) 481–492.
[15] M.B. Fuertes, et al., Type I interferon response and innate immune sensing of cancer, Trends Immunol. 34 (2) (2013) 67–73.
[16] D.L. Burdette, R.E. Vance, STING and the innate immune response to nucleic acids in the cytosol, Nat. Immunol. 14 (1) (2013) 19–26.
[17] H. Ishikawa, Z. Ma, G.N. Barber, STING regulates intracellular DNA-mediated, type I interferon-dependent innate immunity, Nature 461 (7265) (2009) 788–792.
[18] D.L. Burdette, et al., STING is a direct innate immune sensor of cyclic di-GMP, Nature 478 (7370) (2011) 515–518.
[19] L.T. Khoo, L.-Y. Chen, Role of the cGAS-STING pathway in cancer development and oncotherapeutic approaches, EMBO Rep. 19 (12) (2018), e46935.

[20] S. Liu, et al., Phosphorylation of innate immune adaptor proteins MAVS, STING, and TRIF induces IRF3 activation, Science 347 (6227) (2015) aaa2630.
[21] T. Abe, G.N. Barber, Cytosolic-DNA-mediated, STING-dependent proinflammatory gene induction necessitates canonical NF-κB activation through TBK1, J. Virol. 88 (10) (2014) 5328–5341.
[22] Y.A. Hsu, et al., The anti-proliferative effects of type I IFN involve STAT6-mediated regulation of SP1 and BCL6, Cancer Lett. 375 (2) (2016) 303–312.
[23] C. Vanpouille-Box, et al., Cytosolic DNA sensing in organismal tumor control, Cancer Cell 34 (3) (2018) 361–378.
[24] C.H. Tang, et al., Agonist-mediated activation of STING induces apoptosis in malignant B cells, Cancer Res. 76 (8) (2016) 2137–2152.
[25] M.F. Gulen, et al., Signalling strength determines proapoptotic functions of STING, Nat. Commun. 8 (1) (2017), 427.
[26] B. Larkin, et al., Cutting edge: activation of STING in T cells induces type I IFN responses and cell death, J. Immunol. 199 (2) (2017) 397–402.
[27] M.K. Hossain, K.A. Wall, Use of dendritic cell receptors as targets for enhancing anti-cancer immune responses, Cancers 11 (3) (2019) 418.
[28] H. Liu, et al., Nuclear cGAS suppresses DNA repair and promotes tumorigenesis, Nature 563 (7729) (2018) 131–136.
[29] L. Deng, et al., STING-dependent cytosolic DNA sensing promotes radiation-induced type I interferon-dependent antitumor immunity in immunogenic tumors, Immunity 41 (5) (2014) 843–852.
[30] M. Hansen, et al., Cellular based cancer vaccines: type 1 polarization of dendritic cells, Curr. Med. Chem. 19 (25) (2012) 4239–4246.
[31] D. Peng, et al., Epigenetic silencing of TH1-type chemokines shapes tumour immunity and immunotherapy, Nature 527 (7577) (2015) 249–253.
[32] T. Ohkuri, et al., Effects of STING stimulation on macrophages: STING agonists polarize into “classically” or “alternatively” activated macrophages? Hum. Vacc. Immunother. 14 (2) (2018) 285–287.
[33] T. Ohkuri, et al., Intratumoral administration of cGAMP transiently accumulates potent macrophages for anti-tumor immunity at a mouse tumor site, Cancer Immunol. Immunother. 66 (6) (2017) 705–716.
[34] C.D. Mills, et al., M-1/M-2 macrophages and the Th1/Th2 paradigm, J. Immunol. 164 (12) (2000) 6166–6173.
[35] S. Gordon, F.O. Martinez, Alternative activation of macrophages: mechanism and functions, Immunity 32 (5) (2010) 593–604.
[36] O. Demaria, et al., STING activation of tumor endothelial cells initiates spontaneous and therapeutic antitumor immunity, Proc. Natl. Acad. Sci. U. S. A. 112 (50) (2015) 15408–15413.
[37] G.L. Beatty, et al., Exclusion of T cells from pancreatic carcinomas in mice is regulated by Ly6C(low) F4/80(+) extratumoral macrophages, Gastroenterology 149 (1) (2015) 201–210.
[38] H.J. Lee, et al., Tertiary lymphoid structures: prognostic significance and relationship with tumour-infiltrating lymphocytes in triple-negative breast cancer, J. Clin. Pathol. 69 (5) (2016) 422–430.
[39] C. Sautès-Fridman, et al., Tertiary lymphoid structures in cancers: prognostic value, regulation, and manipulation for therapeutic intervention, Front. Immunol. 7 (2016) 407.
[40] D.S. Chen, I. Mellman, Elements of cancer immunity and the cancer-immune set point, Nature 541 (7637) (2017) 321–330.
[41] W.H. Fridman, et al., The immune contexture in cancer prognosis and treatment, Nat. Rev. Clin. Oncol. 14 (12) (2017) 717–734.
[42] K. Mukai, et al., Activation of STING requires palmitoylation at the Golgi, Nat. Commun. 7 (2016) 11932.
[43] J. Conlon, et al., Mouse, but not human STING, binds and signals in response to the vascular disrupting agent 5,6-dimethylxanthenone-4-acetic acid, J. Immunol. 190 (10) (2013) 5216–5225.
[44] L. Corrales, et al., Direct activation of STING in the tumor microenvironment leads to potent and systemic tumor regression and immunity, Cell Rep. 11 (7) (2015) 1018–1030.
[45] P.N. Lara Jr., et al., Randomized phase III placebo-controlled trial of carboplatin and paclitaxel with or without the vascular disrupting agent vadimezan (ASA404) in advanced non-small-cell lung cancer, J. Clin. Oncol. 29 (22) (2011) 2965–2971.
[46] A. Ablasser, et al., cGAS produces a 2′-5′-linked cyclic dinucleotide second messenger that activates STING, Nature 498 (7454) (2013) 380–384.
[47] Elie J. Diner, et al., The innate immune DNA sensor cGAS produces a noncanonical cyclic dinucleotide that activates human STING, Cell Rep. 3 (5) (2013) 1355–1361.
[48] X. Zhang, et al., Cyclic GMP-AMP containing mixed phosphodiester linkages is an endogenous high-affinity ligand for STING, Mol. Cell 51 (2) (2013) 226–235.
[49] B.S. Pan, et al., An orally available non-nucleotide STING agonist with antitumor activity, Science 369 (6506) (2020).
[50] E.N. Chin, et al., Antitumor activity of a systemic STING-activating non-nucleotide cGAMP mimetic, Science 369 (6506) (2020) 993–999.
[51] P. Andersson, C. Ostheimer, Editorial: combinatorial approaches to enhance anti-tumor immunity: focus on immune checkpoint blockade therapy, Front. Immunol. 10 (2019), 2083.
[52] J. Nam, et al., Cancer nanomedicine for combination cancer immunotherapy, Nat. Rev. Mater. 4 (2019) 398–414.
[53] M.J. Ernsting, et al., Factors controlling the pharmacokinetics, biodistribution and intratumoral penetration of nanoparticles, J. Control. Release 172 (3) (2013) 782–794.
[54] H.S. Choi, et al., Renal clearance of quantum dots, Nat. Biotechnol. 25 (10) (2007) 1165–1170.
[55] F. Yuan, et al., Vascular permeability in a human tumor xenograft: molecular size dependence and cutoff size, Cancer Res. 55 (17) (1995) 3752–3756.
[56] D.J. Irvine, et al., Synthetic nanoparticles for vaccines and immunotherapy, Chem. Rev. 115 (19) (2015) 11109–11146.
[57] J.A. Champion, S. Mitragotri, Role of target geometry in phagocytosis, Proc. Natl. Acad. Sci. U. S. A. 103 (13) (2006) 4930–4934.
[58] Y. Geng, et al., Shape effects of filaments versus spherical particles in flow and drug delivery, Nat. Nanotechnol. 2 (4) (2007) 249–255.
[59] J. Shi, et al., Cancer nanomedicine: progress, challenges and opportunities, Nat. Rev. Cancer 17 (1) (2017) 20–37.
[60] C. Théry, S. Amigorena, The cell biology of antigen presentation in dendritic cells, Curr. Opin. Immunol. 13 (1) (2001) 45–51.
[61] T. Zhao, et al., A transistor-like pH nanoprobe for tumour detection and image-guided surgery, Nat. Biomed. Eng. 1 (2016).
[62] X. Ma, et al., Ultra-pH-sensitive nanoprobe library with broad pH tunability and fluorescence emissions, J. Am. Chem. Soc. 136 (31) (2014) 11085–11092.
[63] A.K. Varkouhi, et al., Endosomal escape pathways for delivery of biologicals, J. Control. Release 151 (3) (2011) 220–228.
[64] A.P. Pandey, K.K. Sawant, Polyethylenimine: a versatile, multifunctional non-viral vector for nucleic acid delivery, Mater. Sci. Eng. C 68 (2016) 904–918.
[65] L. Dai, et al., Size/charge changeable acidity-responsive micelleplex for photodynamic-improved PD-L1 immunotherapy with enhanced tumor penetration, Adv. Funct. Mater. 28 (18) (2018) 1707249.
[66] Y. Yan, H. Ding, pH-responsive nanoparticles for cancer immunotherapy: a brief review, Nanomaterials (Basel) 10 (8) (2020).
[67] D. Shae, et al., Endosomolytic polymersomes increase the activity of cyclic dinucleotide STING agonists to enhance cancer immunotherapy, Nat. Nanotechnol. 14 (3) (2019) 269–278.
[68] M. Wehbe, et al., Nanoparticle delivery improves the pharmacokinetic properties of cyclic dinucleotide STING agonists to open a therapeutic window for intravenous administration, J. Control. Release 330 (2021) 1118–1129.
[69] D.C. Nguyen, et al., Amphiphilic polyelectrolyte graft copolymers enhance the activity of cyclic dinucleotide STING agonists, Adv. Healthc. Mater. 10 (2) (2021), e2001056.
[70] Zhang, Y., et al., pH-responsive STING-activating DNA nanovaccines for cancer immunotherapy. Adv. Ther.. n/a(n/a): p. 2000083.
[71] D.R. Wilson, et al., Biodegradable STING agonist nanoparticles for enhanced cancer immunotherapy, Nanomedicine 14 (2) (2018) 237–246.
[72] R. Watkins-Schulz, et al., A microparticle platform for STING-targeted immunotherapy enhances natural killer cell- and CD8(+) T cell-mediated anti-tumor immunity, Biomaterials 205 (2019) 94–105.
[73] X. Lu, et al., Engineered PLGA microparticles for long-term, pulsatile release of STING agonist for cancer immunotherapy, Sci. Transl. Med. 12 (556) (2020).
[74] C. Chen, et al., Cytosolic delivery of thiolated Mn-cGAMP nanovaccine to enhance the antitumor immune responses, Small 17 (19) (2021), e2102241.
[75] M. An, et al., Induction of necrotic cell death and activation of STING in the tumor microenvironment via cationic silica nanoparticles leading to enhanced antitumor immunity, Nanoscale 10 (19) (2018) 9311–9319.
[76] N. Cheng, et al., A nanoparticle-incorporated STING activator enhances antitumor immunity in PD-L1-insensitive models of triple-negative breast cancer, JCI Insight 3 (22) (2018), e120638.
[77] S.T. Koshy, et al., Liposomal delivery enhances immune activation by STING agonists for cancer immunotherapy, Adv. Biosyst. 1 (1–2) (2017) 1600013.
[78] M.C. Hanson, et al., Nanoparticulate STING agonists are potent lymph node-targeted vaccine adjuvants, J. Clin. Invest. 125 (6) (2015) 2532–2546.
[79] H. Miyabe, et al., A new adjuvant delivery system ‘cyclic di-GMP/YSK05 liposome’ for cancer immunotherapy, J. Control. Release 184 (2014) 20–27.
[80] T. Nakamura, et al., Liposomes loaded with a STING pathway ligand, cyclic di-GMP, enhance cancer immunotherapy against metastatic melanoma, J. Control. Release 216 (2015) 149–157.
[81] J. Chen, et al., In situ cancer vaccination using lipidoid nanoparticles, Sci. Adv. (2021) 7(19).
[82] M. Wang, et al., Efficient delivery of genome-editing proteins using bioreducible lipid nanoparticles, Proc. Natl. Acad. Sci. U. S. A. 113 (11) (2016) 2868–2873.
[83] Y. Li, et al., Combinatorial library of chalcogen-containing lipidoids for intracellular delivery of genome-editing proteins, Biomaterials 178 (2018) 652–662.
[84] D.G. Leach, et al., STINGel: controlled release of a cyclic dinucleotide for enhanced cancer immunotherapy, Biomaterials 163 (2018) 67–75.
[85] J.R. Baird, et al., Evaluation of explant responses to STING ligands: personalized Immunosurgical therapy for head and neck squamous cell carcinoma, Cancer Res. 78 (21) (2018) 6308.
[86] C.G. Park, et al., Extended release of perioperative immunotherapy prevents tumor recurrence and eliminates metastases, Sci. Transl. Med. 10 (433) (2018) eaar1916.
[87] D.W. Pack, et al., Design and development of polymers for gene delivery, Nat. Rev. Drug Discov. 4 (7) (2005) 581–593.
[88] R. Rai, S. Alwani, I. Badea, Polymeric nanoparticles in gene therapy: new avenues of design and optimization for delivery applications, Polymers 11 (4) (2019) 745.
[89] E.M. Bachelder, et al., Acetal-derivatized dextran: an acid-responsive biodegradable material for therapeutic applications, J. Am. Chem. Soc. 130 (32) (2008) 10494–10495.
[90] K.E. Broaders, et al., Acetalated dextran is a chemically and biologically tunable material for particulate immunotherapy, Proc. Natl. Acad. Sci. U. S. A. 106 (14) (2009) 5497–5502.

[91] N.P. Restifo, M.E. Dudley, S.A. Rosenberg, Adoptive immunotherapy for cancer: harnessing the T cell response, Nat. Rev. Immunol. 12 (4) (2012) 269–281.
[92] D.N. Kapoor, et al., PLGA: a unique polymer for drug delivery, Ther. Deliv. 6 (1) (2015) 41–58.
[93] M.E. Jacobson, et al., Delivery of 5′-triphosphate RNA with endosomolytic nanoparticles potently activates RIG-I to improve cancer immunotherapy, Biomater. Sci. 7 (2) (2019) 547–559.
[94] D. Wang, et al., Acid-activatable versatile micelleplexes for PD-L1 blockade-enhanced cancer photodynamic immunotherapy, Nano Lett. 16 (9) (2016) 5503–5513.
[95] M. Luo, et al., A STING-activating nanovaccine for cancer immunotherapy, Nat. Nanotechnol. 12 (7) (2017) 648–654.
[96] H. Liu, et al., Structure-based programming of lymph-node targeting in molecular vaccines, Nature 507 (7493) (2014) 519–522.
[97] K. Maisel, et al., Exploiting lymphatic vessels for immunomodulation: rationale, opportunities, and challenges, Adv. Drug Deliv. Rev. 114 (2017) 43–59.
[98] M. Luo, et al., Synergistic STING activation by PC7A nanovaccine and ionizing radiation improves cancer immunotherapy, J. Control. Release 300 (2019) 154–160.
[99] P. Ray, et al., PEG-b-poly (carbonate)-derived nanocarrier platform with pH-responsive properties for pancreatic cancer combination therapy, Colloids Surf. B: Biointerfaces 174 (2019) 126–135.
[100] R.A. Cordeiro, et al., Poly(β-amino ester)-based gene delivery systems: from discovery to therapeutic applications, J. Control. Release 310 (2019) 155–187.
[101] M. Li, et al., Composition design and medical application of liposomes, Eur. J. Med. Chem. 164 (2019) 640–653.
[102] A. Bunker, A. Magarkar, T. Viitala, Rational design of liposomal drug delivery systems, a review: combined experimental and computational studies of lipid membranes, liposomes and their PEGylation, Biochim. Biophys. Acta Biomembr. 1858 (10) (2016) 2334–2352.
[103] M.A. Mintzer, E.E. Simanek, Nonviral vectors for gene delivery, Chem. Rev. 109 (2) (2009) 259–302.
[104] N.-D. Dan, H. James, J.S. Caroline, Structure-activity relationship in cationic lipid mediated gene transfection, Curr. Med. Chem. 10 (14) (2003) 1233–1261.
[105] K. Oumzil, et al., pH-cleavable nucleoside lipids: a new paradigm for controlling the stability of lipid-based delivery systems, ChemMedChem 10 (11) (2015) 1797–1801.
[106] D. Liu, et al., Synthesis and characterization of a series of carbamate-linked cationic lipids for gene delivery, Lipids 40 (8) (2005) 839–848.
[107] C. Robert, et al., Pembrolizumab versus Ipilimumab in Advanced Melanoma, N. Engl. J. Med. 372 (26) (2015) 2521–2532.
[108] R.S. Herbst, et al., Predictive correlates of response to the anti-PD-L1 antibody MPDL3280A in cancer patients, Nature 515 (7528) (2014) 563–567.
[109] J. Larkin, et al., Combined nivolumab and Ipilimumab or monotherapy in untreated melanoma, N. Engl. J. Med. 373 (1) (2015) 23–34.
[110] Y. Sato, et al., A pH-sensitive cationic lipid facilitates the delivery of liposomal siRNA and gene silencing activity in vitro and in vivo, J. Control. Release 163 (3) (2012) 267–276.
[111] K.L. Harper, et al., Mechanism of early dissemination and metastasis in Her2(+) mammary cancer, Nature 540 (7634) (2016) 588–592.
[112] D.S.A. Nuyten, et al., Predicting a local recurrence after breast-conserving therapy by gene expression profiling, Breast Cancer Res. 8 (5) (2006), R62.
[113] R. Narayanaswamy, V.P. Torchilin, Hydrogels and their applications in targeted drug delivery, Molecules 24 (3) (2019) 603.